ACS APPLIED MATERIALS & INTERFACES

Research Article

www.acsami.org

Comparative Interface Metrics for Metal-Free Monolayer-Based Dye-Sensitized Solar Cells

Kung-Ching Liao,[†] Hafeez Anwar,[‡,§] Ian G. Hill,[‡] Grigory K. Vertelov,[†] and Jeffrey Schwartz*[,†]

[†]Department of Chemistry, Princeton University, Princeton, New Jersey 08544, United States

[‡]Department of Physics and Atmospheric Science, Dalhousie University, Halifax, NS B3H4R2 Canada

[§]Department of Physics, University of Agriculture, Faisalabad 38040, Pakistan

Supporting Information

ABSTRACT: The first quantitative comparison between self-assembled monolayers of homologous carboxylate- and phosphonate-terminated organic dyes that are of use in dye-sensitized solar cells (DSSCs) is reported. (Cyanovinyl)-phosphonate-terminated oligothiophenes and (cyanovinyl)carboxylate-terminated oligothiophenes were synthesized on TiO_2 thin film electrodes. Structurally analogous organics were compared for the effect of the anchoring groups on photochemical properties in solution as measured by UV/vis spectroscopy and for reactivity with the electrode surface. Monolayers were grown on the TiO_2 electrodes either by "tethering by aggregation and growth" (T-BAG) or by solution dipping. Surface roughness and homogeneity, elemental composition, and thickness of the monolayers were evaluated by atomic force microscopy (AFM), X-ray photoelectron spectroscopy (XPS), and ellipsometry. Molecular loadings for each monolayer on TiO_2 were quantified by quartz crystal microgravimetry (QCM), and the stability of bonding between each class of dyes and the TiO_2 was evaluated by measuring desorption, also by QCM; the carboxylates underwent significant dissociation in aqueous media but the phosphonates did not. DSSCs were prepared from each congener and from simple oligothiophene phosphonates to determine the effect of the cyanovinyl group on device behavior; all DSSCs were studied under irradiation from a AM 1.5G solar light source; the effect of cyanovinyl group termination was comparable to that of adding a thiophene moiety, and the DSSC using a self-assembled monolayer of (sexithiophene)phosphonate (6TP) had total power conversion efficiency (η) of ca. 5%.

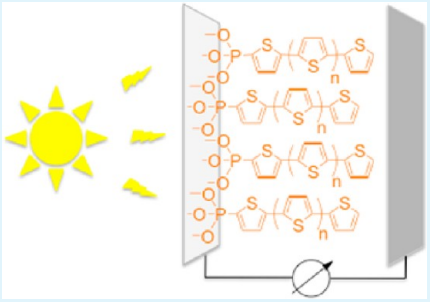

KEYWORDS: *phosphonate self-assembled monolayers, carboxylate self-assembled monolayers, oligothiophenes, precious metal-free dye, dye-sensitized solar cells*

INTRODUCTION

Dye-sensitized solar cells (DSSCs) continue to attract considerable attention as inexpensive alternatives to conventional p-n junction solar cells for the generation of electricity; they do not require high-purity materials and can be implemented at low cost.[1] This type of device typically consists of an n-type wide band gap semiconductor (such as TiO_2) that is deposited onto a transparent conducting oxide (TCO) electrode; dye molecules are adsorbed and anchored onto the semiconductor, and a redox electrolyte matrix is placed in contact with a metallic counter electrode.[2] The best known of these was pioneered by Grätzel and co-workers, who demonstrated that dyes based on organometallic complexes of ruthenium or, less commonly, zinc can achieve high power conversion efficiencies of up to 12.3% under AM 1.5G irradiation.[3,4] From a practical standpoint, however, the high cost and low abundance of ruthenium has lead researchers to consider organic dyes, which have advantages of low cost, high molar extinction coefficients, structural and functional flexibility, and facile preparation and purification.[5,6] It has been proposed[2] that the carboxylate anchor group, either with organic or organometallic moieties, can participate in electron transfer from the photoexcited dye molecule to the semiconductor, and this has been demonstrated experimentally.[7] Other classes of nonmetallic organic dyes have been studied systemically, but only at the theoretical level;[8−12] among these, donor−π−bridge−acceptor organic frameworks have attracted keen interest because of the variety of functional groups that can be incorporated in such dyes.[13]

Self-assembled monolayers of phosphonates (SAMPs) are robust building blocks for surface and interface modification; they are attractive alternatives to organosilicon-[14,15] and organocarboxylate-based[16] coatings where stability to hydrolysis is required. SAMPs can be prepared as highly vertically ordered and dense monolayers. They provide stable and organized platforms for modifying the gate dielectric in organic thin-film transistors,[17−24] construction of SAMP duplexes,[25−29] applications in DNA microarrays,[30] sensing of target molecules in electrolyte-gated field-effect nanowire transistors,[31] and for promoting cell adhesion on oxide and polymer substrates.[32−34]

Received: September 6, 2012
Accepted: November 9, 2012
Published: November 9, 2012

 © 2012 American Chemical Society dx.doi.org/10.1021/am301907z | ACS Appl. Mater. Interfaces 2012, 4, 6735−6746

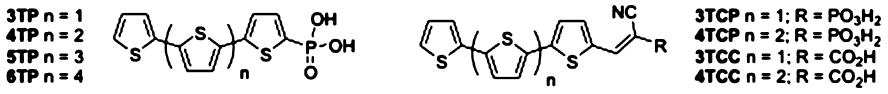

Figure 1. Oligothiophene phosphonate and carboxylate dyes.

Theoretical studies suggest that phosphonate anchoring groups should be comparable to carboxylates for facilitating electron transfer from a surface-bound dye to a semiconductor electrode.[10]

The goal of our study was to quantitatively compare the effect of the more common carboxylate anchoring groups with phosphonate analogs for their effect on photochemical properties in solution as measured by UV/vis spectroscopy and for reactivity with a TiO_2 electrode surface. It was of particular interest to determine molecular loadings for analog monolayers on TiO_2 by quartz crystal microgravimetry (QCM), and to determine, also quantitatively, the stability of these dyes on the TiO_2 in the aqueous media that characterize DSSCs. A notable gap in our understanding of DSSCs is that, although organic dyes absorbed onto TiO_2 surfaces have been characterized by UV/vis absorption spectroscopy, water wetting contact angle measurements, atomic force microscopy (AFM), ellipsometry, or X-ray photoelectron spectroscopy (XPS),[35] for the most part, molecular loadings of such dye molecules have not been measured directly; only in a few cases have indirect measurements of loading been made by desorption of dye molecules from TiO_2 into aqueous ammonia solutions:[36] Lacking measurement of electrode surface loading by the various dyes makes it problematic to meaningfully compare devices based on them. It was also of interest to quantitatively compare the effect of increasing conjugation length in a series of simple oligothiophene dyes achieved by successive introduction of thiophene units on the performance of simple DSSCs with the introduction of terminal cyanoacrylate moieties[5] as polar, electron-withdrawing groups, that are used to shift absorption maxima toward visible wavelength regions of high solar radiation intensity[6,37] and proposed to enhance exciton separation and electron capture by the TiO_2.[38] We report herein results of these quantitative studies, which show that, while molecular loadings of carboxylate and phosphonate analog dyes can be made comparable on TiO_2, carboxylate derivates readily desorb from this surface under aqueous conditions, but the phosphonates do not. We show that SAMPs of simple oligothiophenes on TiO_2 semiconductor electrodes provide DSSCs in which power-conversion efficiency is improved with an increasing number of thiophene units in the dye (**3TP**-**6TP**; Figure 1) as measured under irradiation from a AM 1.5G solar light source; loadings for **3TP**-**6TP** were comparable, so changes in device performance can be attributed directly to changes in oligomer number. We also show the surprising result that the effect of cyanovinyl group termination (**4TCC** and **4TCP**; Figure 1) on DSSC performance is comparable only to that of adding a simple thiophene moiety.

EXPERIMENTAL SECTION

General. α-Terthiophen-2-yl-boronic acid,[39] α-quarterthiophen-2-yl-phosphonic acid[40] (**4TP**), α-terthiophen-2-yl-carboxaldehyde,[41] and α-quarterthiophen-2-yl-carboxaldehyde[42] were synthesized according to published procedures. Bithiophene (2T, Sigma-Aldrich), α-terthiophene (3T, TCI), and 5-(4,4,5,5-tetramethyl-1,3,2-dioxaborolan-2-yl)-2,2′-bithiophene (TCI) were used as received. All other chemicals were purchased from E. Merck, Sigma-Aldrich, Acros, or TCI, and were used without any further purification. Solvents used for reaction, precipitation, and column chromatography were freshly distilled according to standard procedures. All reactions and manipulations were carried out under an argon atmosphere. ^{1}H and ^{13}C nuclear magnetic resonance (NMR) spectra were recorded using a Bruker AVANCE (500 MHz) at 298K. Chemical shift (δ) and coupling constant (J) data are expressed in units of ppm and Hz, respectively. ^{1}H and ^{13}C chemical shifts are referred to the solvent signal. Mass spectrometry was performed on a Kratos MS 50 RFA. UV/vis absorption spectra were recorded on an Agilent-8453 spectrophotometer. Atomic force microscopy (AFM) analysis of films was done using a Digital Instruments Dimension NanoMan equipped with silicon tips in tapping mode. Quartz crystal microbalance (QCM) measurements were made using an International Crystal Manufacturing standard (clock) oscillator equipped with Au-coated electrodes; the surface roughness of TiO_2/Au-coated electrodes was determined by a BET experiment as previously described.[43] Mg Kα (1253.6 eV) radiation was used for X-ray photoelectron spectroscopic (XPS) analysis. TiO_2 thin films were deposited onto ITO, SiO_2/Si, and Au QCM electrodes, respectively, using the method described in our previous reports.[34,44] DSSC J–V characteristics were measured in the dark and under illumination using a Keithley 236 source-measure unit. Illumination was provided by a Newport/Oriel solar simulator equipped with AM1.5G filters. Intensities were measured using a broadband thermopile detector.

α-Oligothiophen-2-yl-phosphonic Acids and (1-Cyano-[α-oligothiophen-2-yl]-vinyl)phosphonic Acids. Syntheses of phosphonic acid diethyl ester precursors to these dyes are found in the Supporting Information. The phosphonic acid diethyl ester (1 mmol) was suspended in anhydrous DCM (20 mL) under an argon atmosphere, and bromotrimethylsilane (0.8 mL, 4 mmol) was added. The reaction mixture was stirred overnight at room temperature; anhydrous methanol (0.8 mL) was then added, and the reaction mixture was stirred for an additional 6 h. The resulting suspension was concentrated under reduced pressure, and the solid was washed thoroughly with DCM (10 mL) and diethyl ether (20 mL), and was recrystallized from methanol and THF, affording the product. Photophysical properties of these compounds are listed in Table 1 and shown in Figure 2.

*(1-Cyano-2-[α-terthiophen-2-yl]-vinyl)phosphonic Acid (**3TCP**).* Dark red solid; yield 90%. ^{1}H NMR (500 MHz, d_6-DMSO, 298K, TMS): δ = 8.04 (d, ^3J (H,P) = 18.5 Hz, 1*H*), 7.87 (d, ^3J (H,H) = 3.5 Hz, 1*H*), 7.61 (d, ^3J (H,H) = 5.0 Hz, 1*H*), 7.55 (d, ^3J (H,H) = 4.0 Hz, 1*H*), 7.55 (d, ^3J (H,H) = 4.0 Hz, 1*H*), 7.45 (d, ^3J (H,H) = 3.0 Hz, 1*H*), 7.38 (d, ^3J (H,H) = 4.0 Hz, 1*H*), 7.15 (dd, ^3J (H,H) = 5.6 Hz, ^3J

Table 1. Photophysical Properties and Comparative Parameters for the Oligothiophene Dyes

dye	λ_{max} (nm)[a]	ε ($\times 10^4$ M^{-1} cm^{-1})[c]	HOMO/LUMO (eV)[d]	band gap (eV)[d]
3TP	357	2.38	−5.40/−2.09	3.31
4TP	395	3.55	−5.17/−2.24	2.93
5TP	421	4.16	−5.04/−-2.33	2.71
6TP	430	4.89	−4.94/−2.38	2.56
3TCP	392 (413)[b]	5.96	−5.53/−2.71	2.82
3TCC	413 (416)[b]	4.23	−5.55/−2.84	2.71
4TCP	413 (438)[b]	6.90	−5.31/−2.75	2.56
4TCC	436 (440)[b]	5.77	−5.32/−2.87	2.45

[a]Absorption of charge-transfer transitions measured in THF. [b]Absorption spectra measured in DMF. [c]ε: absorption coefficient. [d]B3LYP/6-31G(d) calculated values.

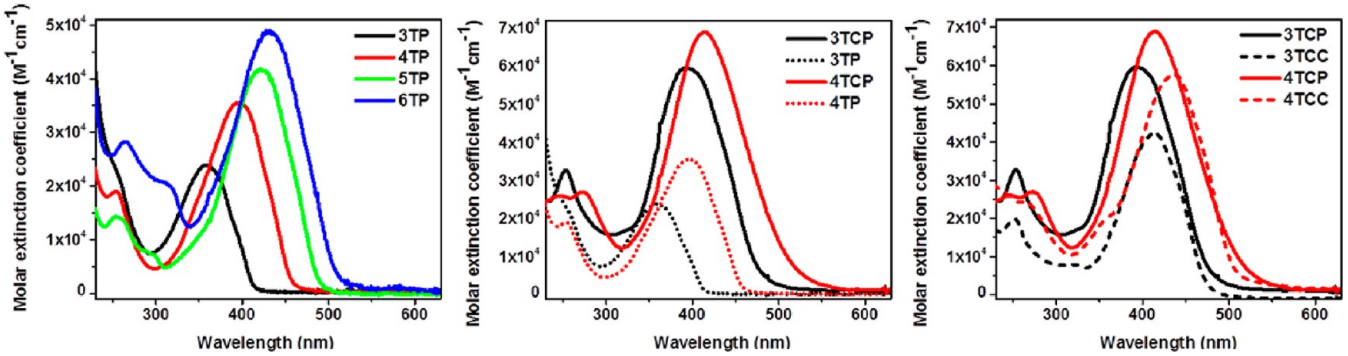

Figure 2. Absorption spectra of (a) **3TP-6TP** in THF; (b) **3TCP**, **3TP**, **4TCP**, and **4TP** in THF comparing (cyanovinyl)oligothiophene phosphonated species with their oligothiophene phosphonated congeners; and (c) absorption spectra of **3TCP**, **3TCC**, **4TCP**, and **4TCC** in THF comparing (cyanovinyl)oligothiophene phosphonated species with (cyanovinyl)oligothiophene carboxylated ones.

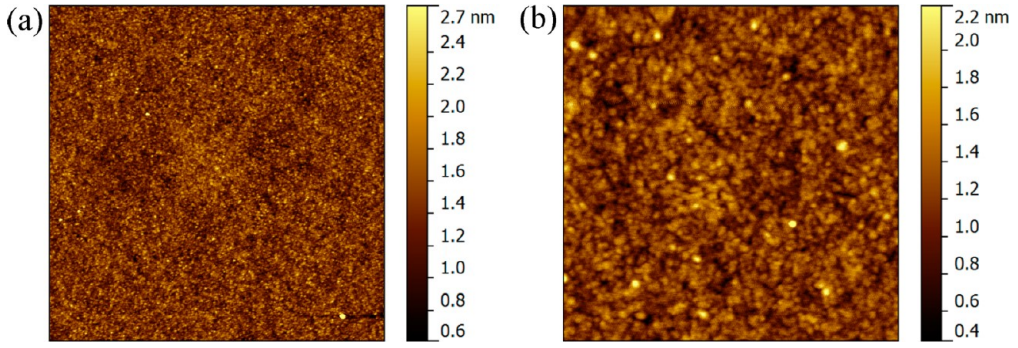

Figure 3. AFM images of 2 nm TiO_2 /SiO_2/Si: (a) 5 μm × 5 μm (rms roughness: 0.28 nm); (b) 1 μm × 1 μm (rms roughness: 0.37 nm).

(H,H) = 4.0 Hz, 1*H*) ppm. ^{13}C NMR (125 MHz, d_6-DMSO, 298K): δ = 146.4, 146.4, 142.9, 139.2, 137.9, 135.6, 135.5, 133.7, 128.8, 127.7, 126.6, 125.5, 125.1, 124.8, 117.3, 117.2, 101.1, 99.6 ppm. ^{31}P NMR (202 MHz, d_6-DMSO, 298K): δ = 5.42 ppm. HRMS (ESI-TOF) for $C_{15}H_{11}NO_3PS_3$: calcd, 379.9639 (M+H) $^+$; found, *m*/*z* 379.9635.

*(1-Cyano-2-[α-Quarterthiophen-2-yl]-vinyl)phosphonic acid (**4TCP**).* Dark red solid; yield 94%. ^{1}H NMR (500 MHz, d_6-DMSO, 298K): δ = 8.02 (d, ^3J (H,P) = 18.5 Hz, 1*H*), 7.87 (d, ^3J (H,H) = 4.0 Hz, 1*H*), 7.58−7.55 (m, 3*H*), 7.42 (d, ^3J (H,H) = 3.5 Hz, 1*H*), 7.41 (d, ^3J (H,H) = 3.0 Hz, 1*H*), 7.38 (dd, ^3J (H,H) = 3.5 Hz, ^3J (H,H) = 1.0 Hz, 1*H*), 7.33 (d, ^3J (H,H) = 4.0 Hz, 1*H*), 7.13 (dd, ^3J (H,H) = 5.0 Hz, ^3J (H,H) = 4.0 Hz, 1*H*) ppm. ^{13}C NMR (125 MHz, d_6-DMSO, 298K): δ = 146.4, 142.8, 139.2, 137.3, 136.4, 135.8, 135.7, 135.6, 134.2, 133.9, 128.6, 127.8, 126.2, 126.1, 125.7, 125.3, 124.9, 124.7, 117.3, 117.2, 101.1, 99.6 ppm. ^{31}P NMR (202 MHz, d_6-DMSO, 298K): δ = 5.49 ppm. HRMS (ESI-TOF) for $C_{19}H_{13}NO_3PS_4$: calcd, 461.9516 (M+H)$^+$; found, *m*/*z* 461.9509.

*α-Terthiophen-2-yl-phosphonic Acid (**3TP**).*[45] Greenish yellow solid; yield 70%. ^{1}H NMR (500 MHz, [D_6]DMSO, 298K, TMS): δ = 7.56 (d, ^3J (H,P) = 5.5 Hz, 1*H*), 7.38−7.35 (m, 4*H*), 7.30 (d, ^3J (H,H) = 3.5 Hz, 1*H*), 7.12 (dd, ^3J (H,H) = 5.0 Hz, ^3J (H,H) = 3.5 Hz, 1*H*) ppm. ^{13}C NMR (125 MHz, [D_6]DMSO, 298K): δ = 141.2, 141.1, 136.4, 135.8, 134.8, 134.7, 134.5, 134.2, 134.2, 132.9, 128.6, 126.2, 126.1, 125.1, 124.7, 124.7, 124.6 ppm. ^{31}P NMR (202 MHz, [D_6]DMSO, 298K): δ = 4.32 ppm. HRMS (ESI-TOF) for $C_{12}H_{10}O_3PS_3$: calcd, 328.9530 (M+H)$^+$; found. *m*/*z* 328.9522.

*α-Quinquethiophen-2-yl-phosphonic Acid (**5TP**).* Orange solid; yield 92%. ^{1}H NMR (500 MHz, d_6-DMSO, 298K, TMS): δ = 7.56 (d, ^3J (H,P) = 5.0 Hz, 1*H*), 7.41 (d, ^3J (H,H) = 4.0 Hz, 1*H*), 7.38−7.34 (m, 7*H*), 7.31 (d, ^3J (H,H) = 4.0 Hz, 1*H*), 7.12 (dd, ^3J (H,H) = 5.0 Hz, ^3J (H,H) = 3.5 Hz, 1*H*) ppm. ^{13}C NMR (125 MHz, d_6-DMSO, 298K): δ = 141.1, 141.0, 135.9, 135.8, 135.7, 135.3, 134.8, 134.7, 134.6, 134.5, 128.6, 126.4, 126.0, 125.8, 125.5, 125.5, 125.4, 125.2, 124.8, 124.8, 124.6 ppm. ^{31}P NMR (202 MHz, d_6-DMSO, 298K): δ = 4.25 ppm. HRMS (ESI-TOF) for $C_{20}H_{14}O_3PS_5$: calcd, 492.9284 (M +H)$^+$; found, *m*/*z* 492.9280.

*α-Sexithiophen-2-yl-phosphonic Acid (**6TP**).* Red solid; yield 98%. ^{1}H NMR (500 MHz, d_6-DMSO, 298K, TMS): δ = 7.57−7.55 (m, 2*H*), 7.51 (d, ^3J (H,H) = 4.0 Hz, 1*H*), 7.48 (d, ^3J (H,H) = 4.0 Hz, 1*H*), 7.47 (d, ^3J (H,H) = 3.5 Hz, 1*H*), 7.43 (dd, ^3J (H,H) = 3.0 Hz, ^3J (H,H) = 3.0 Hz, 1*H*), 7.39−7.36 (m, 5*H*), 7.32 (d, ^3J (H,H) = 4.0 Hz, 1*H*), 7.12 (dd, ^3J (H,H) = 5.0 Hz, ^3J (H,H) = 3.5 Hz, 1*H*) ppm. ^{13}C NMR (125 MHz, d_6-DMSO, 298K): δ = 140.8, 140.7, 136.3, 136.2, 135.8, 135.0, 134.9, 134.9, 134.9, 134.9, 134.8, 134.3, 133.2, 132.7, 129.9, 129.6, 128.6, 128.4, 128.2, 126.7, 126.7, 126.1, 125.8, 125.7, 125.5, 125.2, 125.2, 125.1, 124.6 ppm. ^{31}P NMR (202 MHz, d_6-DMSO, 298K): δ = 4.18 ppm. HRMS (ESI-TOF) for $C_{24}H_{16}O_3PS_6$: calcd, 574.9161 (M+H)$^+$; found, *m*/*z* 574.9153.

Synthesis of 1Cyano-[α-oligothiophen-2-yl]-vinyl)carboxylic Acids. *(1-Cyano-2-[α-terthiophen-2-yl]-vinyl)carboxylic Acid (**3TCC**).*[46] A mixture of α-terthiophen-2-yl-carboxaldehyde (497 mg, 1.8 mmol), 2-cyanoacetic acid (463 mg, 5.4 mmol), and ammonium acetate (55 mg, 1.2 mmol) in glacial acetic acid (10 mL) was refluxed for 3 h under argon. The resulting suspension was concentrated under reduced pressure, and the residue was washed thoroughly with DCM (10 mL) and diethyl ether (20 mL). The recovered solid was recrystallized from methanol and THF, affording the product as a purple solid (476 mg, 77%). ^{1}H NMR (500 MHz, d_6-DMSO, 298K): δ = 8.50 (s, 1*H*), 7.99 (d, ^3J (H,H) = 3.5 Hz, 1*H*), 7.61−7.61 (m, 3*H*), 7.46 (d, ^3J (H,H) = 3.0 Hz, 1*H*), 7.39 (d, ^3J (H,H) = 3.0 Hz, 1*H*), 7.19 (dd, ^3J (H,H) = 4.0 Hz, ^3J (H,H) = 3.5 Hz, 1*H*) ppm. ^{13}C NMR (125 MHz, d_6-DMSO DMSO, 298K): δ = 163.7, 146.5, 145.3, 141.8, 138.5, 135.5, 134.0,133.5, 128.8, 128.3, 126.8, 125.6, 125.3, 125.2, 116.6 ppm. HRMS (ESI-TOF) for $C_{16}H_{10}NO_2S_3$: calcd, 343.9874 (M+H)$^+$; found, *m*/*z* 343.9870.

*(1-Cyano-2-[α-quarterthiophen-2-yl]-vinyl)carboxylic Acid (**4TCC**).* The synthetic procedure was similar to the preparation of **3TCC** via a Knoevenagel reaction using α-quarterthiophen-2-yl-carboxaldehyde (200 mg, 0.56 mmol), cyanoacetic acid (145 mg, 1.68 mmol), ammonium acetate (30 mg, 0.65 mmol), which gave crude product that was recrystallized from methanol and THF, affording a dark red solid (219 mg, 92%). ^{1}H NMR (500 MHz, d_6-DMSO, 298K):

Scheme 1. Synthetic Route to Prepare Cyanovinyl-Conjugated Phosphonate and Carboxylate Dyes[a]

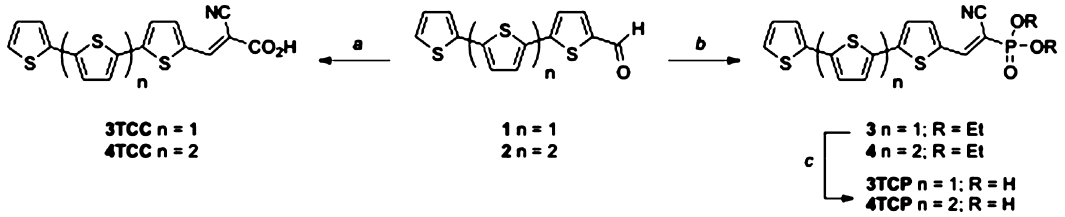

[a]Reagents and conditions: (a) cyanoacetic acid, NH_4OAc, HOAc, reflux, 77% for **3TCC** and 92% for **4TCC**; (b) Diethyl (cyanomethyl)-phosphonate, piperidine, $MeCN/CHCl_3$, reflux, 97% for **3** and 73% for **4**; (c) TMSBr, CH_2Cl_2, then MeOH, 90% for **3TCP** and 94% for **4TCP**.

Scheme 2. Synthetic Route to Prepare the Organic Dyes[a]

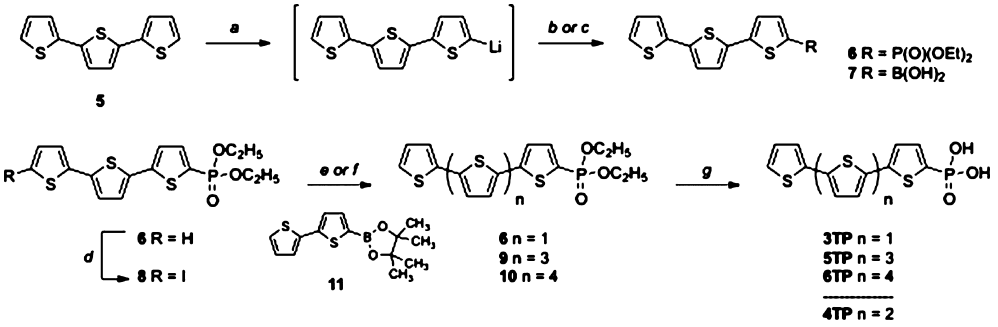

[a]Reagents and conditions: (a) BuLi, THF, −60 °C; (b) $P(O)(OEt)_2Cl$, 87%; (c) $B(OMe)_3$, followed by H_2SO_4, 85%; (d) NIS, I_2, TFA, MeOH, 78%; (e) **7**, $Pd(PPh_3)_4$, Na_2CO_3, THF, H_2O, reflux, 86%; (f) **11**, $Pd(PPh_3)_4$, Na_2CO_3, THF, H_2O, reflux, 10%; (g) TMSBr, CH_2Cl_2, then MeOH. BuLi = butyllithium, THF = tetrahydrofuran, NIS = N-iodosuccinimide, TFA = trifluoroacetic acid, **11** = 5-(4,4,5,5-tetramethyl-1,3,2-dioxaborolan-2-yl)-2,2′-bithophene, TMSBr = bromotrimethylsilane.

δ = 8.27 (s, 1H), 7.83 (d, ^3J (H,H) = 4.0 Hz, 1*H*), 7.56 (d, ^3J (H,H) = 5.0 Hz, 1*H*), 7.54 (d, ^3J (H,H) = 4.0 Hz, 1*H*), 7.54 (d, ^3J (H,H) = 4.0 Hz, 1*H*), 7.40 (dd, ^3J (H,H) = 4.0 Hz, ^3J (H,H) = 3.5 Hz, 1*H*), 7.38 (d, ^3J (H,H) = 3.5 Hz, 1*H*), 7.21 (s, 1*H*), 7.12 (dd, ^3J (H,H) = 5.0 Hz, ^3J (H,H) = 4.0 Hz, 1*H*) ppm. ^{13}C NMR (125 MHz, d_6-DMSO, 298K): δ = 163.0, 137.1, 136.3, 135.8, 135.2, 134.3, 134.1, 128.6, 127.6, 126.2, 126.1, 125.7, 125.2, 125.0, 124.7, 118.0 ppm. HRMS (ESI-TOF) for $C_{20}H_{12}NO_2S_4$: calcd, 425.9751 $(M+H)^+$; found, *m*/*z* 425.9738. Photophysical properties of these compounds are listed in Table 1 and shown in Figure 2.

General Methods for Preparing Self-Assembled Monolayers of Phosphonates (SAMPs) and Carboxylates (SAMCs) on TiO_2 Thin Films. Thin films of TiO_2 deposited onto a SiO_2/Si substrate were used as a model system to study deposition of the oligothiophene and carboxylate- and phosphonate-terminated (cyanovinyl)-oligothiophene dyes on TiO_2 electrodes; the deposition method was adapted from our previous reports,[34,44] and involves thermolysis of metal oxide surface-attached titanium tetra-*tert*-butoxides proceeded by sequential decomposition of *tert*-butoxide groups and cross-linking of the resulting oxide units under controlled heating to form a robust TiO_2 thin film. AFM images of TiO_2 thin films deposited onto Si/SiO_2 revealed a smooth surface with roughness (rms: 0.28 nm) comparable to that of the underlying SiO_2 surface (rms: 0.21 nm) (Figure 3). The detailed surface morphology of the TiO_2 thin film was observed at higher magnification of the AFM image (Figure 3b), which suggests that the thin film consists of an aggregate of TiO_2 nanoparticles of diameters of from 30 to 50 nm; the thickness of the TiO_2 film was estimated by QCM and ellipsometry to be 2.5 nm.[43]

SAMPs of the α-oligothiophen-2-yl phosphonic acids **3TP-6TP** were formed on TiO_2 thin films from a solution in anhydrous THF (1.0 μM) by four cycles of T-BAG treatment[17,40] and heating (120 °C for 1 h under argon). Any residual multilayer was removed after this heating step by solvent rinsing under sonication condition. Negligible changes in QCM frequencies were measured between the second and third T-BAG cycles, so film coverage was considered to be complete at that point. Films prepared under these conditions were surface conforming and had essentially no pin holes as determined by AFM. SAMPs were also formed by immersing the TiO_2 thin films into a solution of α-oligothiophen-2-yl phosphonic acids **3TP-6TP** (0.1 mM) in THF and methanol (1:1) mixture for 48 h, respectively. The dye-absorbed TiO_2 thin-films were then rinsed with isopropanol and dried by a steam of nitrogen. Negligible changes in QCM frequencies were measured after 24 h of immersion, so film coverage was considered to be complete at that point. SAMP film quality was also evaluated by water wetting contact angle (θ), XPS, and QCM analyses. Self-assembled monolayers of (cyanovinyl)phosphonate- and carboxylate-conjugated oligothiophenes **3TCP**, **4TCP**, **3TCC**, and **4TCP** were grown onto the TiO_2 surface in the same way.

Fabrication and Characterization of DSSCs. General fabrication and cell assembly of DSSCs were modified from the procedure published by Grätzel, et al.[47] The photoelectrodes were fabricated by spin coating (1500 rpm, 1 min) a blocking layer of ~25 nm TiO_2 nanoparticles (Evonik Aerodisp W740X) on FTO coated glass. Following drying at 125 °C for 6 min and calcination in air at 450 °C for 30 min, the resulting layer thickness is approximately 1.5 μm. A mixed layer of nano (15−20 nm) and scattering (>100 nm) TiO_2 particles (Solaraonix 18NR-O) was then deposited by screen printing using a 43-thread/cm mesh, and calcined in air at 450 °C for 60 min. Most devices were fabricated in this way; the sintered TiO_2 film could also be further treated with 0.2 M $TiCl_4$ aqueous solution at 70 °C for 30 min, then washed with deionized water and ethanol, and annealed at 500 °C at 30 min. (see Table 3, entry for **6TP**). Then the substrates were cooled to room temperature and immersed into the solution of phosphonate dyes (**3TP-6TP**, **3TCP**, and **4TCP**; 0.1 mM) in a THF and methanol (1:1) mixture or a saturated solution of carboxylate dyes (**3TCC** and **4TCC**; ca. 2 mM) in methanol for 48 h, respectively. The completed photoelectrodes were assembled with a sputtered Pt counter electrode and a 25 μm Surlyn spacer. Predrilled holes in the counter electrode were used to fill the cell with an I^-/I_3^--based electrolyte (Dyesol EL-141). Following filling, the holes were sealed with Surlyn and a microscope coverslip. The active area of the cell, defined by the size of the TiO_2 electrode, was 0.04 cm^2.

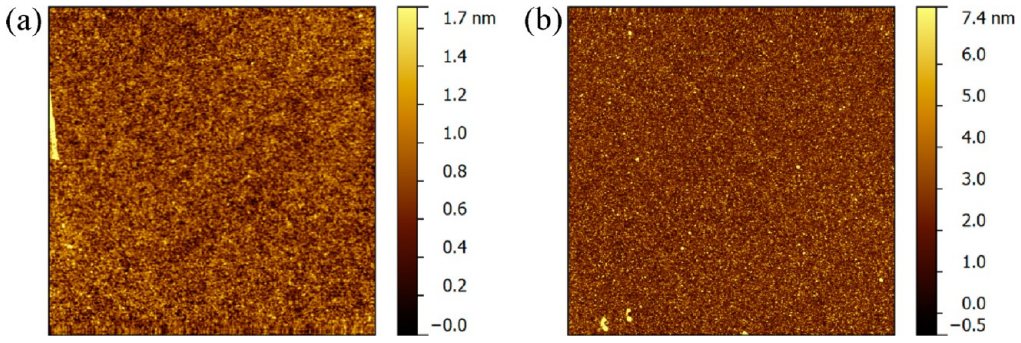

Figure 4. AFM images of (a) 2.0 nm **4TCP**/TiO_2/SiO_2/Si (rms roughness: 0.37 nm); (b) 2.0 nm **4TCC**/TiO_2/SiO_2/Si (rms roughness: 0.42 nm). Scan area is 5 μm × 5 μm.

RESULTS AND DISCUSSION

The synthesis of cyanovinyl-conjugated oligothiophene dyes is shown in Scheme 1. Briefly, **3TCC** and **4TCC** were synthesized from (α-terthiophen-2-yl)carboxaldehyde **1**[41] and (α-quaterthiopen-2-yl)carboxaldehyde **2**,[42] respectively, that were condensed with cyanoacetic acid via an ammonium acetate-catalyzed Knoevenagel reaction.[48] Phosphonate-terminated analogs **3TCP** and **4TCP** were synthesized through piperidine-catalyzed condensation of the aldehyde precursors with diethyl (cyanomethyl)phosphonate followed by hydrolysis of ester intermediates **3** and **4**. As shown in Figure 2, absorption spectra of the carboxylate- and phosphonate-terminated (cyanovinyl)oligothiophene dyes showed a red-shift of their absorption maxima with higher extinction coefficients compared to their simple oligothiophene dye congeners (Table 1); phosphonate-terminated dyes **3TCP** and **4TCP** absorbed at shorter wavelengths, but with larger band widths and higher extinction coefficients compared to their carboxylate analogs **3TCC** and **4TCC**. This is attributed to the effect of the electron-withdrawing propensity provided by the (cyanovinyl)-carboxylate and -phosphonate groups, which also extend the effective conjugation length of the oligothiophene framework.[11] These data are consistent with those experimental and theoretical studies that indicate that carboxylate anchors provide better conjugation than phosphonate ones with their carbon-based chromophores and to induce a greater red-shift in their absorption spectra.[8]

α-Oligothiophen-2-yl phosphonic acids **3TP**, **5TP** and **6TP** were synthesized as shown in Scheme 2; **4TP** was prepared according to our previous report.[40] In brief, the oligothiophenes were constructed via Suzuki coupling[49] in which key intermediate **4** was prepared from α-terthiophene by a sequence of lithiation, substitution by phosphonate, and iodination (overall yield 68%). Sexithiophene **2** was made from **1** and (α-terthiophen-2-yl)boronic acid catalyzed using $Pd(PPh_3)_4$; quinquethiophene **3** was synthesized similarly from **1** and (bithioenyl)boronic ester **11**. The (α-oligothiophen-2-yl)phosphonic acids (**3TP-6TP**) were obtained by bromotrimethylsilane-promoted hydrolysis of their diethyl ester derivatives.[50] Structures of all new compounds were characterized spectroscopically. UV−vis absorption spectra of **3TP-6TP** in THF solution are shown in Figure 6, and parameters, including structure and energy potentials of **3TP-6TP**, were calculated by DFT method (B3LYP/6-31G[d]) and are listed in Table 1. Absorption wavelength maxima (λ_{max}) of **3TP-6TP** displayed a red-shift with increased absorptivity commensurate with the number of thiophene units, which is consistent with increasing the effective conjugation length of the chromophores.[51] The λ_{max} and molar extinction coefficients of **3TP-6TP** (see Table 1) were nearly the same as for the unsubstituted α-oligothiophenes (**3T-6T**),[51] which implies that the phosphonate groups of **3TP-6TP** do not participate strongly in conjugation with the α-oligothiophene motifs.[11]

Deposition and Characterization of (Cyanovinyl)-oligothiophene Phosphonates and Carboxylates on TiO_2. AFM images of **4TCP**/TiO_2/SiO_2/Si (QCM, 0.52 nmol/cm^2; Table 1) prepared by T-BAG (1 μM solution in THF) showed a conforming monolayer with the same homogeneity and surface roughness as the underlying oxide (Figure 4a). The AFM image of T-BAGed **4TCC**/TiO_2/SiO_2/Si (1 μM solution in THF; QCM, 0.55 nmol/cm^2; Table 2) did not show any obvious differences in terms of surface morphology, roughness, or pin holes compared either to the underlying surface or to **4TCP**/TiO_2/SiO_2/Si (Figure 4b). However, unlike the T-BAG, the dipping process did not promote dense packing of the carboxylated derivative when TiO_2 substrates were soaked in a low concentration solution of **4TCC** in THF/methanol (1:1). QCM analysis of **4TCC**/TiO_2 prepared by dipping in a 0.1 mM solution of **4TCC** for 24 h showed the molecular loading to be only 0.04 nmol/cm^2. An approximately 1 order of magnitude higher loading could be obtained by dipping the substrate in a solution of **4TCP** at the same low concentration (0.1 mM; 0.44 nmol/cm^2; Table 2). The molecular loading of **4TCC**/TiO_2 only reached that obtained by T-BAG by using a much higher concentration of **4TCC** solution for dipping (2.0 mM; 0.47 nmol/cm^2; Table 2).

Table 2. Monolayer Characterization Parameters of Phosphonate and Carboxylate Dyes

dye	contact angle (θ)[a]	film thickness (nm)[b]	molecular loading (nmol/cm^2)
3TP	80	1.1	0.64[c] (0.58)[d]
4TP	82	1.5	0.65[c] (0.55)[d]
5TP	76	1.8	0.61[c] (0.49)[d]
6TP	79	2.1	0.62[c] (0.51)[d]
3TCP	76	1.7	0.47[c] (0.41)[d]
3TCC	72	1.8	0.51[c] (0.43)[e]
4TCP	80	2.0	0.52[c] (0.44)[d]
4TCC	70	2.0	0.55[c] (0.47)[e]

[a] θ, water wetting contact angle (deg). [b] Film thickness estimated by ellipsometry. [c] SAMs prepared by the T-BAG method. [d] SAMs prepared by dipping in 0.1 mM in THF. [e] SAMs prepared by dipping in 0.1 mM saturated dye solution (ca. 2 mM in THF).

dx.doi.org/10.1021/am301907z | ACS Appl. Mater. Interfaces 2012, 4, 6735−6746

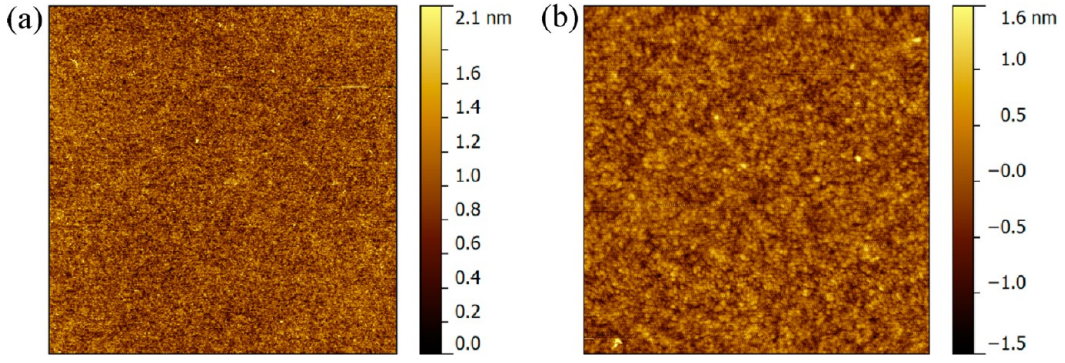

Figure 5. AFM images of 1.5 nm **4TP** /TiO_2/SiO_2/Si: (a) 5 μm × 5 μm (rms roughness: 0.24 nm); (b) 1 μm × 1 μm (rms roughness: 0.38 nm).

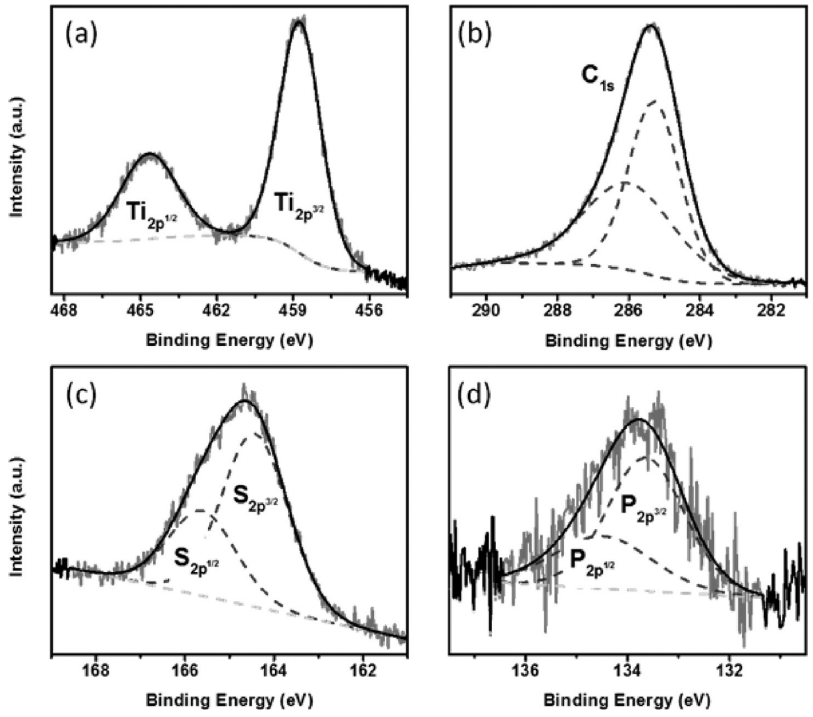

Figure 6. XPS spectra of 1.5 nm **4TP**/TiO_2 (2 nm)/SiO_2/Si. (a) Ti 2p in TiO_2; (b) C 1s in **4TP**; (c) S 2p in **4TP**; (d) P 2p in **4TP**..

This relative reactivity for deposition generally parallels the acidity of phosphonic and carboxylic acids.[52,53] The stability of chemical bonding of phosphonate and carboxylate derivatives was tested by monitoring the change in molecular loading of **4TCP** and **4TCC** on TiO_2 when the substrates were dipped (5 min) and rinsed successively in deionized water and dimethyl sulfoxide (6 cycles of dip and rinse). QCM analysis showed that the molecular loading of **4TCC** on TiO_2 decreased by 28% (from 0.47 to 0.34 nmol/cm^2) in this process, whereas the molecular loading of **4TCP** was reduced by only 6%; this simple test shows that phosphonates provide more stable chemisorption onto TiO_2 than do carboxylates.

Deposition and Characterization of (Oligothiophene)-phosphonate Dyes onto TiO_2. Dense molecular packing of **4TP** on the TiO_2 surface was also accomplished using the T-BAG method and was measured by QCM to be 0.65 nmol/cm^2; this corresponds to a molecular footprint of 25.5 Å^2/molecule and is comparable to our previous measurement of **4TP**/ SiO_2/Si,[40] close to that reported for crystalline 4T.[54] Molecular loadings of **3TP**, **5TP**, and **6TP** were also evaluated by QCM analysis, which gave a molecular footprint similar to the SAMP of **4TP** prepared by the T-BAG method (Table 2). Simply dipping the TiO_2 substrate in a solution of **4TP** did not give SAMP coverage as dense as was prepared by the T-BAG: The molecular packing of the monolayer of **4TP** prepared by this simple dipping was measured by QCM to be only 0.55 nmol/cm^2, which corresponds to a 15% reduction in molecular loading. It may be that disordered packing of molecular constituents of the SAMP results from the dipping process. There was essentially no change in the frequencies (Δf < 5 Hz) of the **4TP**/TiO_2/Au QCM electrodes prepared either from the T-BAG or dipping processes after rinsing sequentially with water, methanol and isopropanol under sonication conditions at 60 °C for 15 min; this observation demonstrates the robustness and stability of the covalent bonding of the phosphonated monolayers to the TiO_2 surface. AFM analysis of SAMPs of **4TP** formed on a TiO_2 thin film by T-BAG showed surface-conforming coverage with rms roughness (0.24 nm) comparable to that of the underlying oxide (0.28 nm), as is expected for a truly surface bound monolayer (Figure 5). The thickness of the **4TP** SAMP was measured by ellipsometry to be 1.5 nm, which is similar to its calculated thickness (1.57 nm)

dx.doi.org/10.1021/am301907z | ACS Appl. Mater. Interfaces 2012, 4, 6735−6746

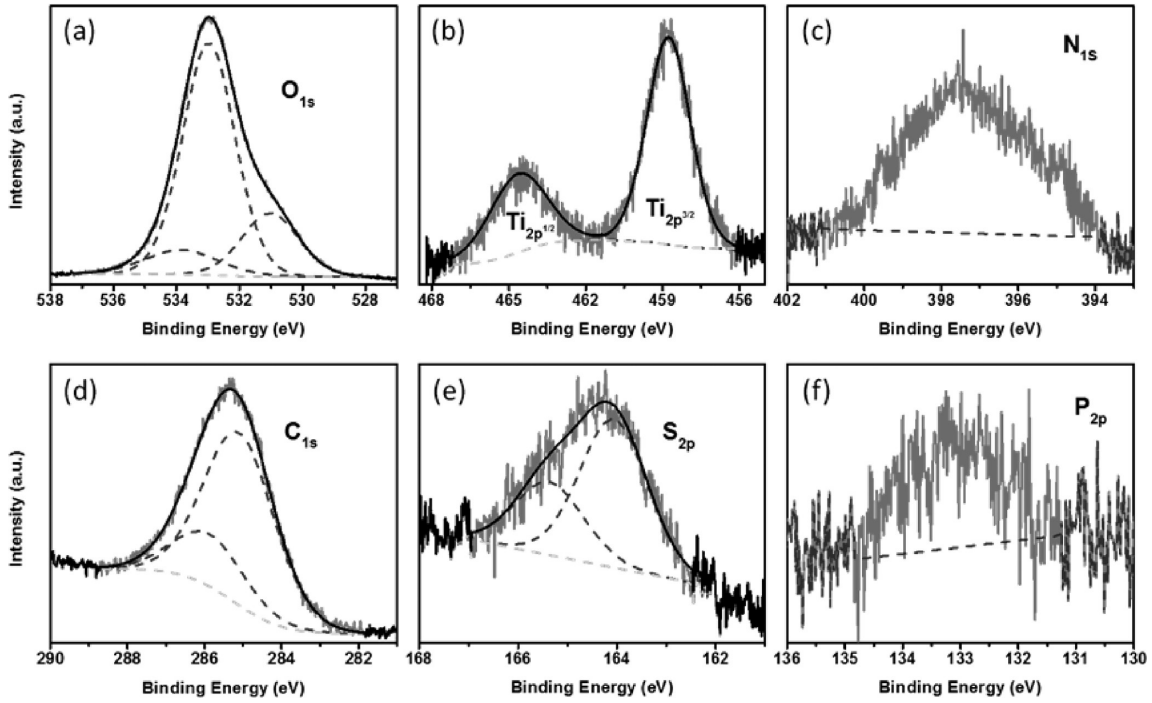

Figure 7. XPS spectra of 2 nm **4TCP**/3 nm TiO_2/SiO_2/Si. (a) O 1s in TiO_2 and SiO_2; (b) Ti 2p in TiO_2; (c) N 1s in **4TCP**; (d) C 1s in **4TCP**; (e) S 2p in **4TCP**; (f) P 2p in **4TCP**..

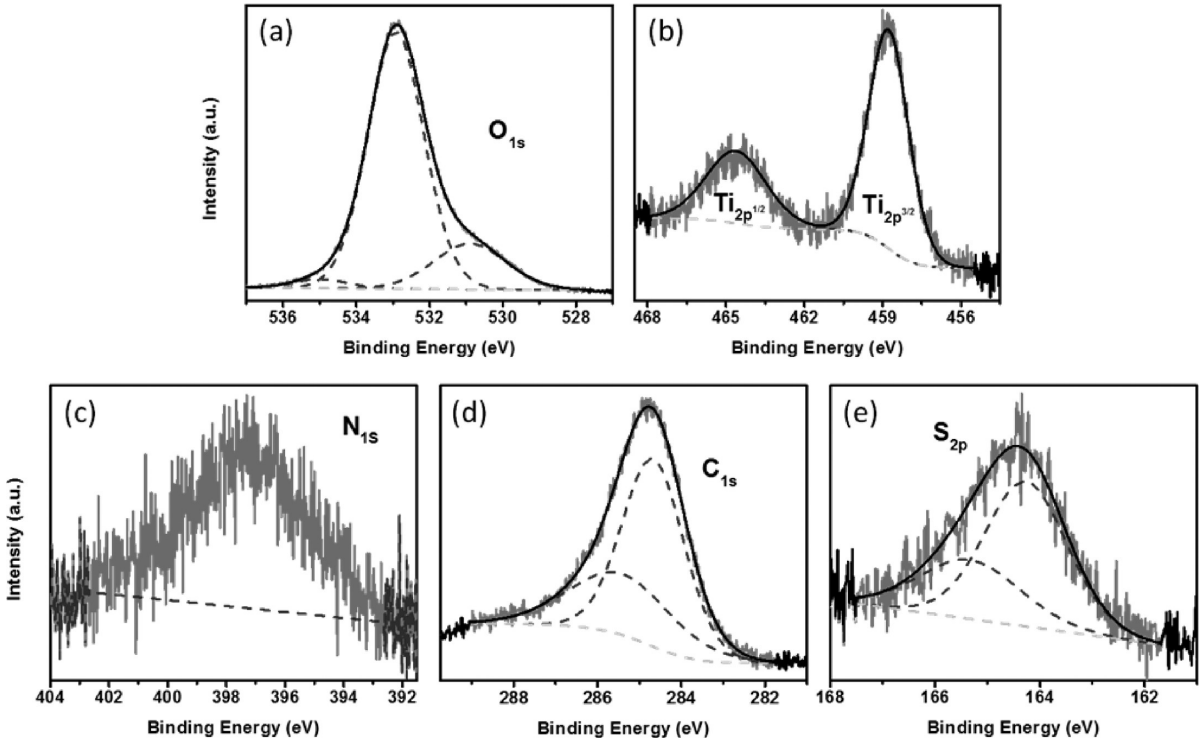

Figure 8. XPS spectra of 2 nm **4TCC**/3 nm TiO_2/SiO_2/Si. (a) O 1s; (b) Ti 2p in TiO_2; (c) N 1s in **4TCC**; (d) C 1s in **4TCC**; (e) S 2p in **4TCC**.

as estimated using the MM2 method in Chem3D software (CambridgeSoft) for **4TP**/TiO_2 in which the C−P bond is normal to the surface; this result is comparable to our previous report of a SAMP of **4TP** that was grown on the SiO_2 surface.[40] The thicknesses of **3TP**, **5TP**, and, **6TP** SAMPs grown on the TiO_2 surface were also measured by ellipsometry and gave 1.1, 1.8, and 2.1 nm, respectively (Table 2). That the measured thicknesses of **3TP**-**6TP** SAMPs were close to their calculated lengths suggests that only small deviations of oligothiophene moieties from a vertical orientation, if any, exist.[40]

XPS Analyses. XPS was used to analyze the elemental composition of the monolayer as well as the underlying TiO_2/SiO_2 substrate. Detailed scans of the O 1s (532.5 eV), Ti 2p (458.8 and 464.5 eV), and Si 2p regions (104.0 eV) are shown in Figure 4 and confirm the presence of Ti on the SiO_2 surface. The O 1s showed a shoulder at lower binding energy compared

dx.doi.org/10.1021/am301907z | ACS Appl. Mater. Interfaces 2012, 4, 6735−6746

to SiO_2 (530.4 eV), attributed to TiO_2. Detailed XPS scans of **4TP**/TiO_2/SiO_2/Si for Ti 2p (458.8 and 464.6 eV), C 1s (285.4 eV), S 2p (164.7 eV), and P 2p (133.8 eV) regions are shown in Figure 6, which confirm the presence of a thiophene phosphonate on the TiO_2 thin film. XPS of C 1s showed a shoulder at higher binding energy (286.1 eV), attributed to the sp^2-hybridized carbons connected to sulfur atom in the oligothiophene phosphonate. The other oligothiophene phosphonate/TiO_2/SiO_2/Si substrates (**3TP**, **5TP**, and **6TP**) were also examined by XPS, which showed results for elemental composition consistent with analogs of **4TP**/TiO_2/SiO_2/Si. The elemental compositions of T-BAGed **4TCC**/TiO_2 and **4TCP**/TiO_2 thin films were studied by XPS. As shown in Figures 6 and 7, detailed XPS scans for **4TCP**/TiO_2 showed elemental compositions similar to **4TP**/TiO_2 for Ti 2p (458.8 and 464.5 eV), C 1s (285.3 eV), S 2p (164.2 eV), and P 2p (133.2 eV) regions, but with an additional signal for N 1s (397.5 eV); the elemental composition for **4TCC**/TiO_2 (Figure 8) was also examined by XPS, which was similar to that for **4TCP**/TiO_2 for the Ti 2p (458.8 and 464.7 eV), C 1s (284.8 eV), S 2p (164.4 eV), and N 1s (397.2 eV) regions.

Device Performance of DSSCs Using Oligothiophene SAMPs, and a Comparison with Carboxylate Analogs. Parameters for dye-sensitized solar cells (DSSCs) fabricated with oligothiophene phosphonates **3TP**-**6TP** (open-circuit photovoltage (V_{oc}); short circuit current (J_{sc}); fill factor (FF); and total power conversion efficiency (η), measured under AM 1.5G solar light source (100 mW cm)) are listed in Table 3;

Table 3. DSSC Performance Parameters of Phosphonate and Carboxylate Dyes

dye	V_{OC}[a] (V)	J_{SC}[a] (mA/cm^2)	FF[a] (%)	η[a,b] (%)
3TP	0.43	1.27	54	0.29
4TP	0.47	3.14	48	0.69
5TP	0.57	7.21	61	2.5
6TP	0.58	12.22	59	4.1; 5.0[c]
3TCP	0.53	5.44	48	1.4
3TCC	0.48	2.86	51	0.69
4TCP	0.57	6.93	58	2.3
4TCC	0.50	5.47	61	1.7

[a] V_{oc}, open-circuit photovoltage; J_{sc}, short-circuit photocurrent density; ff, fill factor; and η, total power conversion efficiency. [b] DSSCs were irradiated under 1.0 sun (AM 1.5G) and measured in a 0.04 cm^2 working area on a FTO (8 Ω square^{-1}) substrate. [c] TiO_2 first treated with $TiCl_4$.

photocurrent–voltage (J–V) plots are shown in Figure 9. It is interesting that the open-circuit photovoltage of DSSCs fabricated with oligothiophene phosphonates **3TP**-**6TP** by the dipping process increased monotonically from 0.43 to 0.60 V with the number of thiophene units in the dye. Moreover, the short circuit current and total power conversion efficiency of **3TP**-**6TP** solar cells increased exponentially with the number of thiophene units. Surface molecular loadings for each SAMP were comparable; device performance improved as λ_{max} for the oligothiophene adsorption shifted toward the wavelength of highest emission intensity in the solar radiation spectrum (Figure 2). The λ_{max} of **6TP** (430 nm) is still to the blue of this wavelength (ca. 530 nm). The performance of the DSSC based on **6TP** is likely attributed to the dense molecular loading of the phosphonate molecules in its SAMP (and each has a high molar extinction coefficient); this DSSC showed higher total power conversion efficiency (in which η could be as high as 5%) than did those based on (oligothiophene)carboxylate and -dicarboxylate dyes that were reported to have an even greater number of conjugated thiophene units (for 8T, η = 1.39%; and 12T, η = 0.55%).[55]

DSSCs fabricated from (cyanovinyl)phosphonate (**4TCP**) showed excellent device behavior; 2.3% total power conversion efficiency was obtained (under 1 sun), which compares favorably with other quarterthiophene (4T) derivatives: The efficiencies of **4TCP** DSSCs were more than 50 and 200% greater than those for **4TCC** and **4TP** DSSCs, respectively (Figure 10b). We interpret these results to correlate with the solution absorption spectra of the 4T dyes themselves, in which **4TCP** absorbs with a larger bandwidth (full bandwidth at half height, ca. 100 nm) and higher extinction coefficient ($\varepsilon = 6.9 \times 10^4$ M^{-1} cm^{-1}) compared to its carboxylate (**4TCC**) or simple quarterthiophene phosphonate (**4TP**) analogs, even though **4TP** adsorbed with slightly higher molecular loading (0.55 nmol/cm^2) onto TiO_2 compared to **4TCP** (0.44 nmol/cm^2) or **4TCC** (0.47 nmol/cm^2). Terthiophene (3T) dyes also showed the same trend: Device efficiency of 3T DSSCs was **3TCP** > **3TCC** > **3TP** (Figure 10a), which parallels light absorption of the 3T dyes in terms of λ_{max}, bandwidths, and extinction coefficients.

Performance Analysis of DSSCs. Understanding the short circuit currents and open circuit voltages of our **nTP**-based DSSCs requires analysis of several fundamental photophysical processes. The open circuit voltages of all devices described here are significantly less than the optical gap energies of the dyes. The maximum possible V_{oc} of a DSSC is determined by the difference in energies between the quasi-Fermi level of the TiO_2 (the energy of the electron following charge transfer) and the electrolyte redox potential (here, I^-/I_3^-);[56,57] this assumes that the dye LUMO level is sufficiently above the TiO_2 conduction band and the redox potential is sufficiently above the dye HOMO to allow for electron transfer. The electron affinity of anatase TiO_2 is reported to be ca. 4.0 eV,[58,59] and the redox potential of I^-/I_3^- is 4.8 eV (0.35 V relative to NHE).[59] Thus, regardless of the optical gap of the dye, the maximum V_{oc} that can be produced is ~0.8 V using a TiO_2 electrode and this electrolyte. For instance, while **6TP** exhibits an onset of optical absorption near 540 nm (2.3 eV), the measured V_{oc} at 1 sun is only ~0.6 V. This phenomenon has be noted for other dyes, such as N3,[60] which has an optical gap of ~1.7 eV but results in typical DSSCs V_{oc} values of ~0.6–0.8 V under 1 sun illumination; our results are consistent with this model.

Although an upper limit exists for V_{oc}, an illuminated cell can produce a lower V_{oc} than this estimated maximum. Typically, V_{oc} increases with increasing illumination or, more accurately, with increasing photocurrent density.[57] Our data show a monotonic increase in V_{oc} and an accompanying increase in J_{sc} with increasing conjugation length for the **nTP** series of dyes. We suggest that this observed increase in V_{oc} is due to the increase in photocurrent (produced at the same illumination) as the conjugation length of the dye is increased. In particular, in simple solar cell models, a photocurrent source (I_p) is placed in parallel with an ideal diode.[61] The magnitude of I_p is a linear function of illumination. Under open circuit conditions, all of the photocurrent, I_p, must pass through the ideal diode, and the diode current must equal the photocurrent. Based on the Shockley diode eq 1 it is expected that V_{oc} increases as the logarithm of the photocurrent.[57,61] Using the short circuit current density as a proxy for the photocurrent, we find that V_{oc}

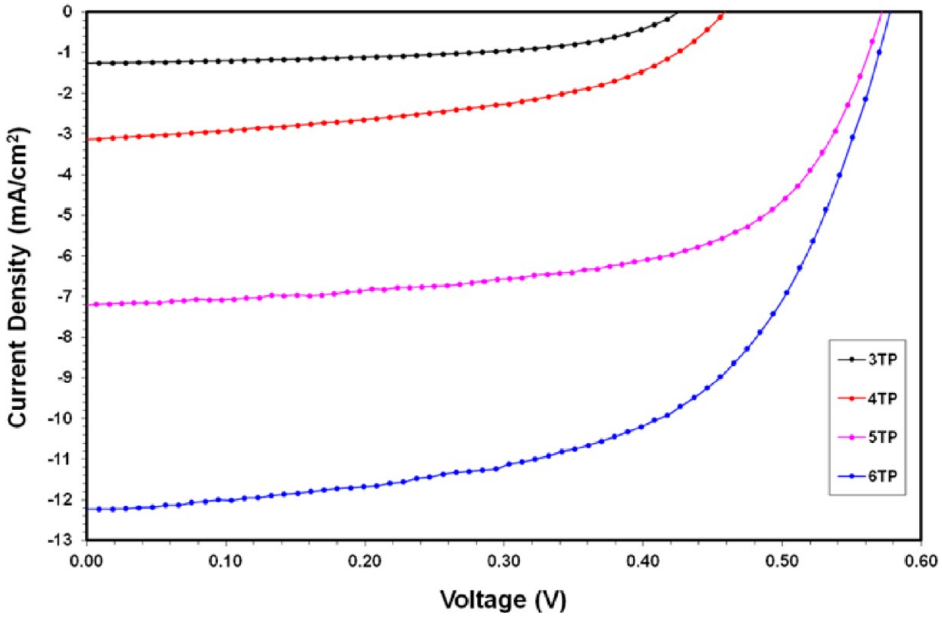

Figure 9. Photocurrent density–voltage plot for **3TP-6TP** DSSCs showing systematic improvement with increasing number of thiophene units.

does indeed scale as the logarithm of the photocurrent, indicating that the observed change in V_{oc} with an increasing number of thiophene rings is due to the increased photocurrent density.

$$I_p = I_s(e^{qV_{oc}/nk_BT} - 1) \text{ or } V_{oc} \approx \frac{nk_BT}{q}\ln\left(\frac{I_p}{I_s}\right) \text{ for } \frac{qV_{oc}}{nk_BT} \gg 1 \quad (1)$$

Diode reverse saturation current, I_s; electronic charge, q; ideality factor, n; Boltzmann's constant, k_B; temperature, T.

The strong relationship between the short circuit current density and the number of thiophene units in the dye reveals an interesting facet of photophysics that pertains to series of congener dyes that differ not only in band gap but also in molecular size. As seen in Table 3, the current density approximately doubles with each additional thiophene unit. As expected, the peak molar extinction coefficient increases as the number of thiophene rings also increases, and absorption spectra red-shift toward the maximum of the solar spectrum, near 530 nm (Figure 2). Thus, all other structural factors being equal, we would expect that the current produced by these devices will increase as thiophene rings are added to the dye. To estimate the difference in photocurrent due to the change in absorption spectra, we consider the FTO-coated glass substrate to have a hard short-wavelength cutoff at 350 nm, and the photocurrent is assumed to be proportional to the product of the absorption spectrum (Figure 2) and a blackbody spectrum at 5777 K integrated between 350 nm and the optical absorption onset wavelength for each dye species. As seen from the data in Table 3, this simple model underestimates the photocurrent increase that is measured: It predicts a 2-fold increase in photocurrent from **4TP** to **6TP**, but a 4-fold increase is observed in experiment.

The simple model described above is flawed in that it implicitly assumes that changing the conjugation length of the molecule has no effect on three important rate factors: (1) electron transfer from the excited dye molecule to the TiO_2; (2) charge recombination from the TiO_2 conduction band to the electrolyte; and, (3) charge recombination from the TiO_2 directly to the oxidized dye. Clearly, all three of these rates have an impact on the observed photocurrent that is measured external to the cell. While we cannot definitively assess the relative importance of each of these three effects, it is reasonable to propose that all will be affected by changing the molecular length of the **nTP** dye as **n** increases (see Table 2), and that all three will tend to increase the photocurrent with increasing conjugation length beyond that which is predicted by the simple model for several reasons. First, the electron affinity of the dye molecule will increase as its conjugation length increases; this decreases the energy difference between the excited state of the dye and the TiO_2 conduction band, which should increase the rate of electron transfer from the dye to the TiO_2[62,63] thus giving rise to a corresponding increase in photocurrent, as electron transfer competes with decay of the excited dye to the ground state. Second, the increase in molecular length of the dye will also effectively increase the tunneling barrier width for an electron in the TiO_2 conduction band to recombine with the electrolyte. Finally, because of the polarity of the **nTP** molecules imparted by the electronegative phosphonate groups, we anticipate that the hole state on the oxidized dye molecule should tend to be localized at its distal end. Thus, the longer the molecule (see Table 2), the lower the probability of direct recombination of an electron from the TiO_2 conduction band and the electrolyte. We believe that these effects, in addition to the commonly discussed overlap of absorption and solar spectra, give rise to the exponential increase in short circuit current density with conjugation length that we have observed.

CONCLUSIONS

A series of metal- and amine-free organic sensitizers based on oligothiophenes and (cyanovinyl)-terminated oligothiophenes was prepared through straightforward synthesis. Structural analysis of dye/TiO_2 substrates was made by QCM, AFM, and XPS and indicated homogeneous growth of monolayers, with no multilayer formation, from (oligothiophene)phosphonates, (cyanovinyl)carboxylate-terminated oligothiophenes, and (cyanovinyl)phosphonate-terminated oligothiophenes. QCM

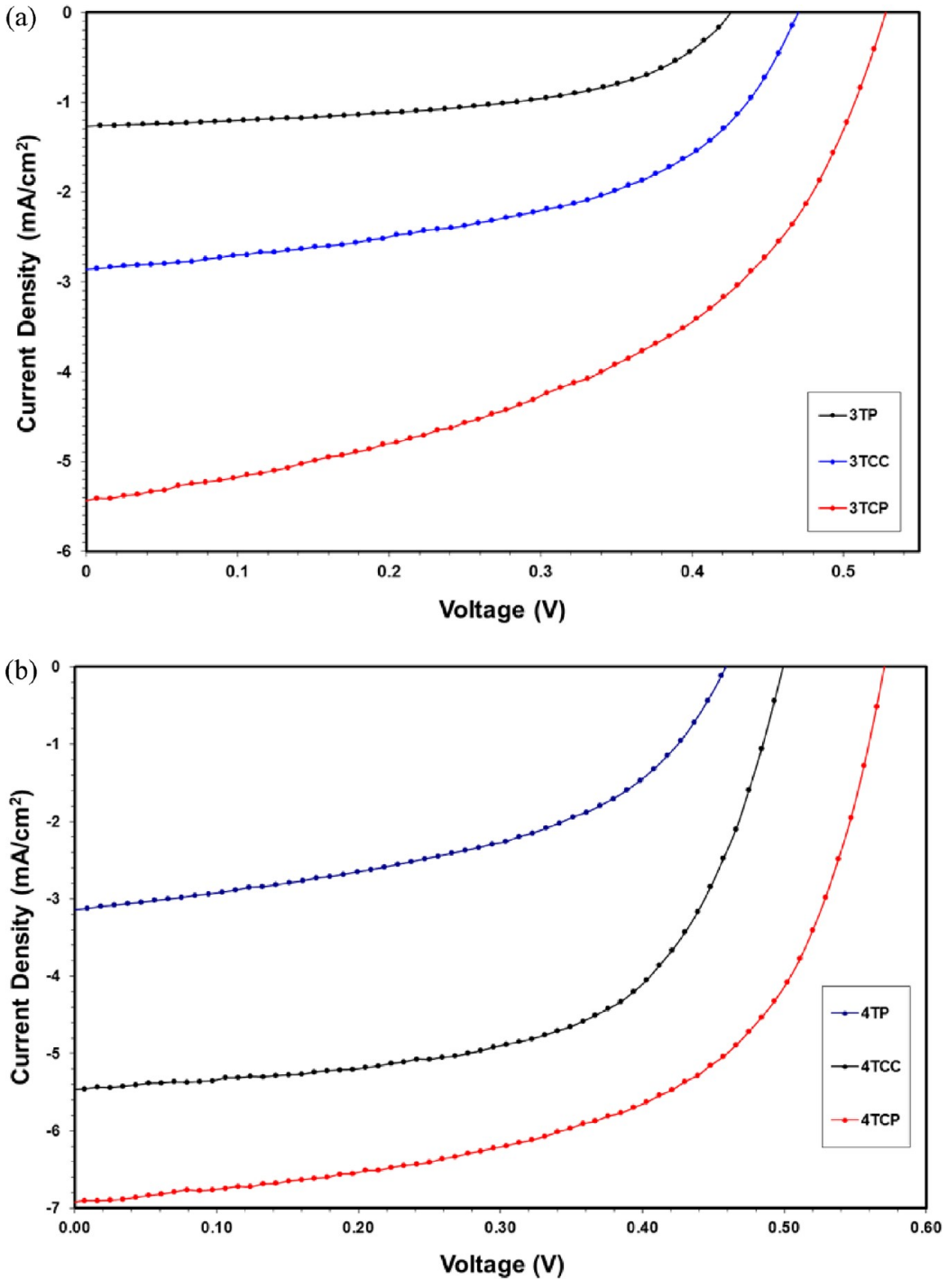

Figure 10. Photocurrent–voltage plot for (a) **3TP**, **3TCC**, and **3TCP**; (b) **4TP**, **4TCC**, and **4TCP** DSSCs showing systematic improvement with changes in terminal groups TCP > TCC > TP.

showed that the T-BAG method gave dense molecular loadings of self-assembled monolayers of phosphonates and carboxylates prepared from 1 μM solutions; adsorption of carboxylate dyes onto TiO_2 by a simple solution dipping process required concentrations of two to 3 orders of magnitude greater, and was thus limited by the solubility of the free dye. The carboxylates experienced significant dissociation in aqueous media, whereas the phosphonates did not. All were shown to be effective light-absorbing chromophores for use in DSSCs; the (cyanovinyl)phosphonate-terminated oligothiophenes showed broader light absorption spectra with higher extinction coefficients compared to their carboxylate-terminated analogs, which correlates with the better performance in DSSCs measured for phosphonate- vs analogous carboxylate-terminated dyes; clearly, UV/vis spectra are one important parameter for predicting device behavior. In general DSSC performance increased commensurately with the conjugation length of the oligothiophene moieties, but it was surprising that the effect of π-extension of conjugated oligothiophene moieties by introduction of the polar cyanovinyl group was only approximately equal to that of one additional thiophene unit (Figure 11). Taken together, the homogeneity of molecular

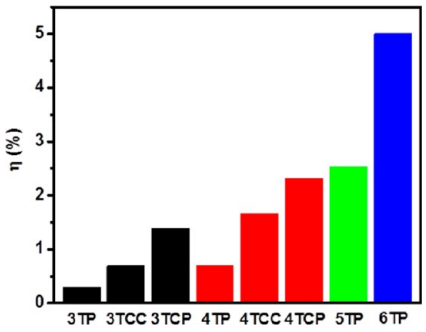

Figure 11. Comparative DSSC device performance of (oligothiophene)phosphonate, (cyanovinyl)phosphonate, and (cyanovinyl)carboxylate dyes.

growth, the high absorptivity onto TiO_2, and the stability of the SAMPs to desorption under aqueous conditions suggest that the phosphonate anchor can be an important constituent in the design of new organic molecular chromophores with wide band absorbance in the visible and near-infrared regions, where a robust interface enabling dense molecular packing onto an oxide semiconductor is essential for DSSC performance.

■ ASSOCIATED CONTENT

Ⓢ Supporting Information

Synthesis of phosphonic acid diethyl ester precursors, ^{1}H, ^{13}C and ^{31}P NMR spectra for all phosphonic and carboxylic acids, and a table of λ_{max} of **3TCP**, **3TCC**, **4TCP**, and **4TCC** measured in several solvents. This material is available free of charge via the Internet at http://pubs.acs.org or from the authors.

■ AUTHOR INFORMATION

Corresponding Author

*E-mail: jschwart@princeton.edu.

Notes

The authors declare no competing financial interest.

■ ACKNOWLEDGMENTS

This work was supported by the Natural Sciences and Engineering Research Council of Canada, the Canada Foundation for Innovation (9584, 11100, 19994), the NSERC Photovoltaic Innovation Network, the National Science Foundation (CHE-0924104), and the Princeton MRSEC of the National Science Foundation (DMR-0819860). K.-C.L. acknowledges support from a Government Fellowship for Study Abroad, from the Ministry of Education, Taiwan. H.A. acknowledges support from the University of Agriculture, Faisalabad, Pakistan, under the Faculty Development Program (FDP) and Higher Education Commission (HEC) of Pakistan.

■ REFERENCES

(1) O'Regan, B.; Grätzel, M. *Nature* **1991**, *353*, 737−740.
(2) Ardo, S.; Meyer, G. J. *Chem. Soc. Rev.* **2009**, *38*, 115−164.
(3) Yella, A.; Lee, H. W.; Tsao, H. N.; Yi, C. Y.; Chandiran, A. K.; Nazeeruddin, M. K.; Diau, E. W. G.; Yeh, C. Y.; Zakeeruddin, S. M.; Grätzel, M. *Science* **2011**, *334*, 629−634.
(4) Gao, F.; Wang, Y.; Shi, D.; Zhang, J.; Wang, M. K.; Jing, X. Y.; Humphry-Baker, R.; Wang, P.; Zakeeruddin, S. M.; Grätzel, M. *J. Am. Chem. Soc.* **2008**, *130*, 10720−10728.
(5) Mishra, A.; Fischer, M. K. R.; Bauerle, P. *Angew. Chem., Int. Ed.* **2009**, *48*, 2474−2499.
(6) Yen, Y. S.; Chou, H. H.; Chen, Y. C.; Hsu, C. Y.; Lin, J. T. *J. Mater. Chem.* **2012**, *22*, 8734−8747.
(7) Hagfeldt, A.; Boschloo, G.; Sun, L.; Kloo, L.; Pettersson, H. *Chem. Rev.* **2010**, *110*, 6595−6663.
(8) Ernstorfer, R.; Gundlach, L.; Felber, S.; Storck, W.; Eichberger, R.; Willig, F. *J. Phys. Chem. B* **2006**, *110*, 25383−25391.
(9) Nilsing, M.; Persson, P.; Lunell, S.; Ojamae, L. *J. Phys. Chem. C* **2007**, *111*, 12116−12123.
(10) Ambrosio, F.; Martsinovich, N.; Troisi, A. *J. Phys. Chem. C* **2012**, *116*, 2622−2629.
(11) Chen, R. K.; Yang, X. C.; Tian, H. N.; Wang, X. N.; Hagfeldt, A.; Sun, L. C. *Chem. Mater.* **2007**, *19*, 4007−4015.
(12) Mulhern, K. R.; Orchard, A.; Watson, D. F.; Detty, M. R. *Langmuir* **2012**, *28*, 7071−7082.
(13) Kitamura, T.; Ikeda, M.; Shigaki, K.; Inoue, T.; Anderson, N. A.; Ai, X.; Lian, T. Q.; Yanagida, S. *Chem. Mater.* **2004**, *16*, 1806−1812.
(14) Aswal, D. K.; Lenfant, S.; Guerin, D.; Yakhmi, J. V.; Vuillaume, D. *Anal. Chim. Acta* **2006**, *568*, 84−108.
(15) Onclin, S.; Ravoo, B. J.; Reinhoudt, D. N. *Angew. Chem., Int. Ed.* **2005**, *44*, 6282−6304.
(16) DiBenedetto, S. A.; Facchetti, A.; Ratner, M. A.; Marks, T. J. *Adv. Mater.* **2009**, *21*, 1407−1433.
(17) Liao, K.-C.; Ismail, A. G.; Kreplak, L.; Schwartz, J.; Hill, I. G. *Adv. Mater.* **2010**, *22*, 3081−3085.
(18) McDermott, J. E.; McDowell, M.; Hill, I. G.; Hwang, J.; Kahn, A.; Bernasek, S. L.; Schwartz, J. *J. Phys. Chem. A* **2007**, *111*, 12333−12338.
(19) McDowell, M.; Hill, I. G.; McDermott, J. E.; Bernasek, S. L.; Schwartz, J. *Appl. Phys. Lett.* **2006**, *88*, 073505.
(20) Ma, H.; Acton, O.; Ting, G.; Ka, J. W.; Yip, H.-L.; Tucker, N.; Schofield, R.; Jen, A. K. Y. *Appl. Phys. Lett.* **2008**, *92*, 113303.
(21) Chung, Y.; Verploegen, E.; Vailionis, A.; Sun, Y.; Nishi, Y.; Murmann, B.; Bao, Z. *Nano Lett.* **2011**, *11*, 1161−1165.
(22) Acton, O.; Ting, G.; Ma, H.; Ka, J. W.; Yip, H.-L.; Tucker, N. M.; Jen, A. K. Y. *Adv. Mater.* **2008**, *20*, 3697−3701.
(23) Burkhardt, M.; Jedaa, A.; Novak, M.; Ebel, A.; Voïtchovsky, K.; Stellacci, F.; Hirsch, A.; Halik, M. *Adv. Mater.* **2010**, *22*, 2525−2528.
(24) Zschieschang, U.; Ante, F.; Schloerholz, M.; Schmidt, M.; Kern, K.; Klauk, H. *Adv. Mater.* **2010**, *22*, 4489−4493.
(25) Cattani-Scholz, A.; Liao, K.-C.; Bora, A.; Pathak, A.; Krautloher, M.; Nickel, B.; Schwartz, J.; Tornow, M.; Abstreiter, G. *Angew. Chem., Int. Ed* **2011**, *50*, A11−A16.
(26) Cattani-Scholz, A.; Liao, K.-C.; Bora, A.; Pathak, A.; Hundschell, C.; Nickel, B.; Schwartz, J.; Abstreiter, G.; Tornow, M. *Langmuir* **2012**, *28*, 7889−7896.
(27) Putvinski, T. M.; Schilling, M. L.; Katz, H. E.; Chidsey, C. E. D.; Mujsce, A. M.; Emerson, A. B. *Langmuir* **1990**, *6*, 1567−1571.
(28) Cao, G.; Hong, H. G.; Mallouk, T. E. *Acc. Chem. Res.* **1992**, *25*, 420−427.
(29) Marcon, R. O.; Brochsztain, S. *Thin Solid Films* **2005**, *492*, 30−34.
(30) Cattani-Scholz, A.; Pedone, D.; Blobner, F.; Abstreiter, G.; Schwartz, J.; Tornow, M.; Andruzzi, L. *Biomacromolecules* **2009**, *10*, 489−496.
(31) Cattani-Scholz, A.; Pedone, D.; Dubey, M.; Neppl, S.; Nickel, B.; Feulner, P.; Schwartz, J.; Abstreiter, G.; Tornow, M. *ACS Nano* **2008**, *2*, 1653−1660.
(32) Danahy, M. P.; Avaltroni, M. J.; Midwood, K. S.; Schwarzbauer, J. E.; Schwartz, J. *Langmuir* **2004**, *20*, 5333−5337.
(33) Dennes, T. J.; Hunt, G. C.; Schwarzbauer, J. E.; Schwartz, J. *J. Am. Chem. Soc.* **2007**, *129*, 93−97.
(34) Dennes, T. J.; Schwartz, J. *J. Am. Chem. Soc.* **2009**, *131*, 3456−3457.
(35) Rensmo, H.; Westermark, K.; Sodergren, S.; Kohle, O.; Persson, P.; Lunell, S.; Siegbahn, H. *J. Chem. Phys.* **1999**, *111*, 2744−2750.
(36) Wu, K.-L.; Li, C.-H.; Chi, Y.; Clifford, J. N.; Cabau, L.; Palomares, E.; Cheng, Y.-M.; Pan, H.-A.; Chou, P.-T. *J. Am. Chem. Soc.* **2012**, *134*, 7488−7496.

(37) Miyazaki, E.; Okanishi, T.; Suzuki, Y.; Ishine, N.; Mori, H.; Takimiya, K.; Harima, Y. *Bull. Chem. Soc. Jpn.* **2011**, *84*, 459−465.
(38) Modelli, A.; Burrow, P. D. *J. Phys. Chem. A* **2011**, *115*, 1100−1107.
(39) Liu, X. M.; Xu, J. M.; He, C. B. *Tetrahedron Lett.* **2004**, *45*, 1507−1510.
(40) Hanson, E. L.; Schwartz, J.; Nickel, B.; Koch, N.; Danisman, M. F. *J. Am. Chem. Soc.* **2003**, *125*, 16074−16080.
(41) Kagan, J.; Arora, S. K. *J. Org. Chem.* **1983**, *48*, 4317−4320.
(42) Yassar, A.; Videlot, C.; Jaafari, A. *Sol. Energy Mater. Sol. Cells* **2006**, *90*, 916−922.
(43) Carolus, M. D.; Bernasek, S. L.; Schwartz, J. *Langmuir* **2005**, *21*, 4236−4239.
(44) Dennes, T. J.; Schwartz, J. *ACS Appl. Mater. Interfaces* **2009**, *1*, 2119−2122.
(45) Hsu, C.-W.; Wang, L.; Su, W.-F. *J. Colloid Interface Sci.* **2009**, *329*, 182−187.
(46) Won, Y. S.; Yang, Y. S.; Kim, J. H.; Ryu, J.-H.; Kim, K. K.; Park, S. S. *Energy Fuels* **2010**, *24*, 3676−3681.
(47) Ito, S.; Murakami, T. N.; Comte, P.; Liska, P.; Grätzel, C.; Nazeeruddin, M. K.; Grätzel, M. *Thin Solid Films* **2008**, *516*, 4613−4619.
(48) Knoevenagel, E. *Chem. Ber.* **1898**, *31*, 2596−2619.
(49) Miyaura, N.; Suzuki, A. *Chem. Rev.* **1995**, *95*, 2457−2483.
(50) Demmer, C. S.; Krogsgaard-Larsen, N.; Bunch, L. *Chem. Rev.* **2011**, *111*, 7981−8006.
(51) Tour, J. M.; Wu, R. L. *Macromolecules* **1992**, *25*, 1901−1907.
(52) Hau, S. K.; Cheng, Y.-J.; Yip, H.-L.; Zhang, Y.; Ma, H.; Jen, A. K. Y. *ACS Appl. Mater. Interfaces* **2010**, *2*, 1892−1902.
(53) Montalti, M.; Wadhwa, S.; Kim, W. Y.; Kipp, R. A.; Schmehl, R. H. *Inorg. Chem.* **1999**, *39*, 76−84.
(54) Sassella, A.; Borghesi, A.; Tubino, R.; Destri, S.; Porzio, W.; Barbarella, G. *Synth. Met.* **2000**, *115*, 69−73.
(55) Tanaka, K.; Takimiya, K.; Otsubo, T.; Kawabuchi, K.; Kajihara, S.; Harima, Y. *Chem. Lett.* **2006**, *35*, 592−593.
(56) Hagfeldt, A.; Grätzel, M. *Acc. Chem. Res.* **2000**, *33*, 269−277.
(57) Grätzel, M. *J. Photochem. Photobiol. C* **2003**, *4*, 145−153.
(58) Könenkamp, R. *Phys. Rev. B* **2000**, *61*, 11057−11064.
(59) Nattestad, A.; Mozer, A. J.; Fischer, M. K. R.; Cheng, Y.-B.; Mishra, A.; Bäuerle, P.; Bach, U. *Nat. Mater.* **2010**, *9*, 31−35.
(60) Chen, K.-S.; Liu, W.-H.; Wang, Y.-H.; Lai, C.-H.; Chou, P.-T.; Lee, G.-H.; Chen, K.; Chen, H.-Y.; Chi, Y.; Tung, F.-C. *Adv. Funct. Mater.* **2007**, *17*, 2964−2974.
(61) Sze, S., M. *Physics of Semiconductor Devices*, 2nd ed.; John Wiley & Sons: New York, 1981.
(62) Lee, J.-J.; Coia, G. M.; Lewis, N. S. *J. Phys. Chem. B* **2004**, *108*, 5269−5281.
(63) Clifford, J. N.; Martinez-Ferrero, E.; Viterisi, A.; Palomares, E. *Chem. Soc. Rev.* **2011**, *40*, 1635−1646.